

Far Ultraviolet Fluorescence of Molecular Hydrogen in IC 63¹

Mark Hurwitz

Space Sciences Laboratory

University of California, Berkeley, California 94720-5030

ABSTRACT

We present observations of H₂ fluorescence at wavelengths between 1000 and 1200 Å from the bright reflection nebula IC 63. Observations were performed with the Berkeley spectrograph aboard the ORFEUS-II mission (Hurwitz et al. 1998). To the best of our knowledge, this is the first detection of astrophysical H₂ fluorescent emission at these wavelengths (excluding planetary atmospheres). The shape of the spectrum is well described by the model of Sternberg (1989). The absolute intensity, however, is fainter than an extrapolation from observations at longer ultraviolet wavelengths (Witt et al. 1989) by a factor of ten. Of the mechanisms that might help reconcile these observations, optical depth effects in the fluorescing H₂ itself are the most promising (or at least the most difficult to rule out).

Subject headings: molecular processes, ISM: molecules, reflection nebulae: individual (IC 63), ultraviolet: ISM

1. INTRODUCTION

In many environments, the equilibrium abundance of the hydrogen molecule (H₂) is determined by a balance between formation on dust grains and photodissociation pumped by photons at wavelengths below about 1108 Å (Shull & Beckwith 1982). Photons between this threshold energy and the Lyman limit populate a large number of rovibrational states in the $B^1\Sigma_u^+$ and $C^1\Pi_u$ electronic levels. En route back to the $X^1\Sigma_g^+$ level, the excited H₂ may radiate through any of several bound-bound and/or bound-free channels leading to a complex fluorescence emission spectrum.

Located about 20' or 1.3 pc from γ Cas, dense gas in the reflection nebula IC 63 is illuminated by a bright UV radiation field. Line widths of a variety of molecular species are quite narrow (Jansen, van Dishoeck, & Black 1994), suggesting that shock excitation is comparatively unimportant in this environment. The nebula provides an excellent test case for models of H₂ fluorescence and other photochemical processes (Jansen et al. 1995).

The fluorescence model described in Sternberg (1988) and Sternberg (1989) has been successfully applied in the interpretation of infrared H₂ fluorescence from the reflection nebulae IC 63 and IC 59 (Luhman et al. 1997), and to the ultraviolet fluorescence in the band near 1600 Å from IC 63 (Sternberg

¹Based on the development and utilization of ORFEUS (Orbiting and Retrievable Far and Extreme Ultraviolet Spectrometers), a collaboration of the Astronomical Institute of the University of Tübingen, the Space Astrophysics Group of the University of California at Berkeley, and the Landessternwarte Heidelberg.

1989) and the Taurus molecular cloud (Hurwitz 1994). In this work we test the model in a previously unexplored band deep in the ultraviolet where the significant majority of the radiated fluorescent power is expected to emerge.

2. OBSERVATIONS AND DATA REDUCTION

The Berkeley EUV/FUV spectrometer, located at the prime focus of the 1-m ORFEUS telescope, flew aboard the space platform *ASTRO-SPAS* during the 1996 November/December mission of the space shuttle *Columbia*. The ORFEUS project and the *ASTRO-SPAS* platform are described in Grewing et al. (1991), while performance of the Berkeley spectrometer during this, its second flight, is discussed in Hurwitz et al. (1998). For reference, the effective area peaks at about 9 cm^2 ; the resolution $\lambda/\Delta\lambda = 3000$ over the 390–1200 Å band.

IC 63 was observed twice, for a total of 3211 sec. The target coordinates were $\alpha = 00^{\circ} 59' 01.29''$, $\delta = +60^{\circ} 53' 17.90''$ (J2000). Absolute positioning of the 26 " diameter ORFEUS entrance aperture is accurate to $\pm 5''$. This location is coincident with that used by Witt et al. (1989) during previous observations with the IUE. We can find no measurement of the nebular proper motion in the literature, but if it is comparable to that of γ Cas, the cumulative motion in the decade since the IUE observations should be well below one arcsecond.

Detector background is estimated from nonilluminated regions above and below the dispersed spectrum. Stray light creates a high background level between 900 and about 1000 Å, limiting the utility of the data for very faint sources such as IC 63. Diffuse “airglow” (including geocoronal/interplanetary emission) is scaled from an off-axis aperture displaced by 2.6 ' from the primary aperture. Statistical and systematic errors associated with background and airglow subtraction are properly tracked. As a final step, we bin the data on 1 Å centers.

The observed spectrum (solid line) and 1σ error (dotted line) are shown in the upper panel of Fig. 1.

3. MODELING OF THE CONTINUUM AND FLUORESCENCE SPECTRUM

To model the observed spectrum, we assume that the intrinsic emission consists of a linear continuum plus the reference far ultraviolet H₂ fluorescence spectrum from Sternberg (1989). The important physical parameters on which Sternberg’s reference spectrum is based are: a nebular density of 100 cm^{-3} , a temperature of 100 K, and an incident UV continuum flux of $3.4 \times 10^{-6} \text{ photons cm}^{-2} \text{ s}^{-1} \text{ Hz}^{-1}$ at 1000 Å (about $100 \times$ the typical interstellar value). The model predicts that the relative strengths of the UV emission features are comparatively unaffected by the detailed parameter values. The strength of the Werner emission features relative to those from the Lyman electronic level varies somewhat with the shape of the incident radiation field, but the dependency is a weak one. Our software accommodates a fixed foreground reddening, using the standard interstellar extinction curve (Cardelli, Clayton, & Mathis 1989, with $R_V = 3.1$). The two free parameters of the fit are the unreddened H₂ scale factor, and the unreddened continuum level at 1000 Å. We fix the (reddened) continuum at 1275 Å to the value observed previously ($3.6 \times 10^{-6} \text{ ergs cm}^{-2} \text{ s}^{-1} \text{ sr}^{-1} \text{ Å}^{-1}$) (Witt et al. 1989). Higher-order polynomial continua did not significantly improve the quality of the fit. Our normalization for the unreddened H₂ scale factor follows Sternberg; a scale factor of unity corresponds to a total UV fluorescent flux of $1.1 \times 10^{-4} \text{ ergs cm}^{-2}$

$\text{s}^{-1} \text{ sr}^{-1}$.

It is important to be cognizant that the sum of the UV fluorescent line strengths in the tabulation of Sternberg (1989) does not equal 1000 in the normalized units adopted in that work. The text states that the tabulation represents the 260 brightest lines, but only after manually coadding the line fluxes did we discover that their summed contribution comprises only 45.6% of the total radiated power. In this work we assume that the weaker lines follow the spectral distribution of the stronger ones, and simply scale the Sternberg reference spectrum upward to account for the missing flux, which is reasonable (Sternberg private communication). We were not aware of the need for this renormalization factor during our analysis of the emission from the Taurus molecular cloud (Hurwitz 1994). In that work we noted that the interstellar radiation field was too faint (by a factor of two) to excite the observed H_2 fluorescence; the renormalization factor neatly resolves this puzzle.

Returning now to IC 63, we note that the column density of interstellar H I toward the nearby illuminating star γ Cas is about $1.5 \times 10^{20} \text{ cm}^{-2}$ (Diplas & Savage 1994). Foreground molecular gas is negligible (Jenkins, private communication). With the usual reddening vs. H I relationship (Bohlin, Savage, & Drake 1978), E_{B-V} is about 0.03 magnitudes. We adopt this foreground reddening for IC 63 as well. In fitting the model to the data, we exclude a few wavelength bins where strong gas phase interstellar absorption is likely to be present, e.g. bins near Lyman β , C II 1036.3 Å, and N II 1084 Å.

Our best-fit model is illustrated in the upper panel of Figure 1 (dashed line). Detailed parameters and confidence intervals (Lampton, Margon, & Bowyer 1976) are illustrated in the lower panel. The reduced χ^2 is about 1.4 at best fit.

4. DISCUSSION

The far ultraviolet continuum from IC 63 will be discussed in a separate work (Gordon & Hurwitz, in prep). Here we focus our attention on the H_2 fluorescence.

Apart from the region longward of 1170 Å, where the data reveal emission features that we have not been able to identify, the general appearance of the model fluorescent spectrum is in good agreement with our observational data in the 1000 – 1200 Å region. The absolute scaling of the fluorescence, however, differs significantly from the values found previously. Witt et al. measured a flux of about $7.5 \times 10^{-4} \text{ ergs cm}^{-2} \text{ s}^{-1} \text{ sr}^{-1}$ between 1350 and 1650 Å. Adopting the line strengths from Sternberg, we find that the IUE band encompasses 26% of the radiated UV power, leading to a total UV flux of about $2.9 \times 10^{-3} \text{ ergs cm}^{-2} \text{ s}^{-1} \text{ sr}^{-1}$, or equivalently, an H_2 scale factor of 26.

This is an observational limit based on what we will refer to as the IUE-band flux, and includes the effects of reddening. For comparison with our dereddened constraints shown in Figure 1, we must remember to deredden the IUE band as well, leading to an H_2 scale factor of about 31 (if $E_{B-V} = 0.03$) in the IUE band. We find a best fit H_2 scale factor of about 3.3 in the ORFEUS band, and a 95% confidence range from 2.2 to 3.9. Our measurements fall an order of magnitude or more below the IUE-band results.

Interestingly, there was some evidence for a shortfall in the measured flux compared to the fluorescence model within the IUE spectrum. In Figure 2 of Witt et al. (1989) it can be seen that the data are below the model at wavelengths below about 1300 Å. The general IUE flux level at ~ 1200 Å would produce about $0.0025 \text{ ph cm}^{-2} \text{ s}^{-1} \text{ Å}^{-1}$ in the ORFEUS aperture, in good agreement with our own measurements. The faintness of the short wavelength IUE data has engendered little previous commentary, perhaps because of

the perception that correction for Lyman α emission and/or stray starlight introduced too much uncertainty at the shortest IUE wavelengths.

Most of the IUE spectrum is dominated by Lyman band transitions to high vibrational states. The ORFEUS spectrum includes both Lyman and Werner features; the latter generally form the most prominent complexes. We have fit the ORFEUS spectrum with varying ratios of Lyman and Werner band line fluxes, but the goodness of fit does not improve measurably. Gross distortions (e.g. complete exclusion of the Werner band) fit the data very poorly, and even at this extremum the ORFEUS spectrum requires an H_2 scale factor no greater than 6.

The IUE aperture ($10 \times 20''$) was somewhat smaller than that used with ORFEUS. Since neither instrument provides useful spatial information within the field of view, both might underestimate the true specific intensity if the fluorescence region is very centrally concentrated. Our larger aperture makes us more susceptible to dilution effects, which could introduce a factor of up to 2.6 in the comparison of our results with those of IUE. We note however that other tracers of central concentration in IC 63 would not predict a strong fall-off in the fluorescent intensity until significantly larger angular scales are reached (Luhman et al. 1997; Jansen, van Dishoeck, & Black 1994). If the general IR-to-UV ratio is comparable to that predicted by Sternberg, the measurements of Luhman et al. (1997) suggest that the dilution within their $74''$ beam was no worse than a factor of ~ 4 , e.g. that the fluorescent region is unlikely to be much smaller than 30 or $40''$ in diameter.

An increase in the dust extinction to which the fluorescent spectrum is subjected could preferentially attenuate the shorter wavelengths, helping to reconcile our results with those of Witt et al.. Complete reconciliation of the ORFEUS and IUE-band by this effect would require roughly 1.5 magnitudes of visual extinction. Given the low extinction toward γ Cas, general interstellar dust is unlikely to be responsible. The nebula itself contains an ample supply of dust; significant differential extinction could arise if the fluorescence region is hidden behind gas that is presumably in atomic form. There are two difficulties with this scenario. The absorbing slab would increase the unreddened H_2 scale factor to about 130, requiring an incident radiation field well in excess of that from γ Cas. Furthermore the infrared fluorescent line intensities (which are far less affected by extinction) would be much brighter than those observed (Luhman et al. 1997).

The H_2 emission spectrum from 1140 to 1680 \AA excited by 100 eV electron impact has recently been published (Liu et al. 1995). J. Ajello kindly provided these data, and the spectrum from 1200 to 1720 \AA produced by 16 eV electrons, in electronic format. The higher energy electron impact spectrum shares some overlap with the ORFEUS spectral band, but the observational data do not enable us to distinguish this process from ordinary photon fluorescence. The “hardness ratio,” here defined as the $1220 - 1300 \text{\AA}$ flux divided by the flux longward of 1400\AA , is comparable for the photon fluorescence spectrum and the 16 eV electron impact spectrum. The 100 eV spectrum is about 50% harder. The electron excitation mechanism thus does not appear to offer a great advantage in reconciling the ORFEUS spectrum with that of IUE. Extension of the electron impact spectra to shorter wavelengths (and probably to lower electron energies) would nonetheless be of utility.

The potential for absorption from quiescent H_2 seems plausible in this environment, but its signature (a series of bands at wavelengths below 1108\AA) is not evident in the spectrum. All of the fluorescent features in the ORFEUS band, not merely those below 1108\AA , are weak compared to the IUE lines.

Witt et al. (1989) predicted that the fluorescent emission at shorter wavelengths would be fainter than the model predictions, invoking optical depth effects within the fluorescent zone itself. The model

of Sternberg includes the effect of dust and gas on the incident radiation field, and properly treats dust extinction as the fluorescent photons exit the cloud. It is “optically thin,” however, in that the outgoing radiation is not subjected to absorption from the rovibrationally excited H₂, a process that becomes increasingly important at shorter wavelengths. Even if the interaction is primarily a resonant scattering, photon trapping will burden the shorter wavelength photons with a longer effective path length and therefore a higher effective extinction before they can escape. This mechanism should convert a fraction of the stellar radiation field into an “excess” of infrared emission (compared to models where the effect is not included). The observed infrared emission from IC 63 exceeds the total incident stellar power (Jansen, van Dishoeck, & Black 1994), so we can say only that the data do not rule out the possibility of this reprocessing effect.

5. CONCLUSIONS

We have detected H₂ fluorescence at wavelengths between 1000 and 1200 Å from the bright reflection nebula IC 63 with the Berkeley spectrograph aboard the ORFEUS-II mission (Hurwitz et al. 1998). The wavelengths and relative strengths of the fluorescent features within the ORFEUS band agree well with the predictions of the model of Sternberg (1989). The absolute fluorescent intensity is fainter than an extrapolation from observations at longer ultraviolet wavelengths (Witt et al. 1989) by a factor of ten. The measurements can not be reconciled by differential extinction from a foreground slab of dust (presumably associated with neutral gas) nor by absorption from quiescent H₂. Optical depth effects in the fluorescing H₂ itself, predicted by Witt et al. (1989), remain the most plausible mechanism to explain our observations.

We acknowledge our colleagues on the ORFEUS team and the many NASA and DARA personnel who helped make the ORFEUS-II mission successful. This work is supported by NASA grant NAG5-696.

REFERENCES

Bohlin, R. C., Savage, B. D., & Drake, J. F. 1978, *ApJ*, 224, 132

Cardelli, J., Clayton, G., & Mathis, J. 1989, *ApJ*, 345, 245

Diplas, A., & Savage, B. D. 1994, *ApJS*, 93, 211

Grewing, M., et al. 1991, in *Extreme Ultraviolet Astronomy*, ed. R. F. Malina & S. Bowyer (Elmsford: Pergamon), 437

Hurwitz, M. 1994, *ApJ*, 433, 149

Hurwitz, M., et al. 1998, *ApJ*

Jansen, D. J., van Dishoeck, E. F., & Black, J. H. 1994, *A&A*, 282, 605

Jansen, D. J., van Dishoeck, E. F., Black, J. H., Spaans, M., & Sosin, C. 1995, *A&A*, 302, 223

Lampton, M., Margon, B., & Bowyer, S. 1976, *ApJ*, 208, 177

Liu, X., Ahmed, S. M., Multari, R. A., James, G. K., & Ajello, J. M. 1995, *ApJS*, 101, 375

Luhman, M. L., Luhman, K. L., Benedict, T., Jaffe, D. T., & Fischer, J. 1997, *ApJ*, 480, L133

Shull, M., & Beckwith, S. 1982, *ARA&A*, 20, 163

Sternberg, A. 1988, *ApJ*, 332, 400

Sternberg, A. 1989, *ApJ*, 347, 863

Witt, A. N., Stecher, T. P., Boroson, T. A., & Bohlin, R. C. 1989, *ApJ*, 336, L21

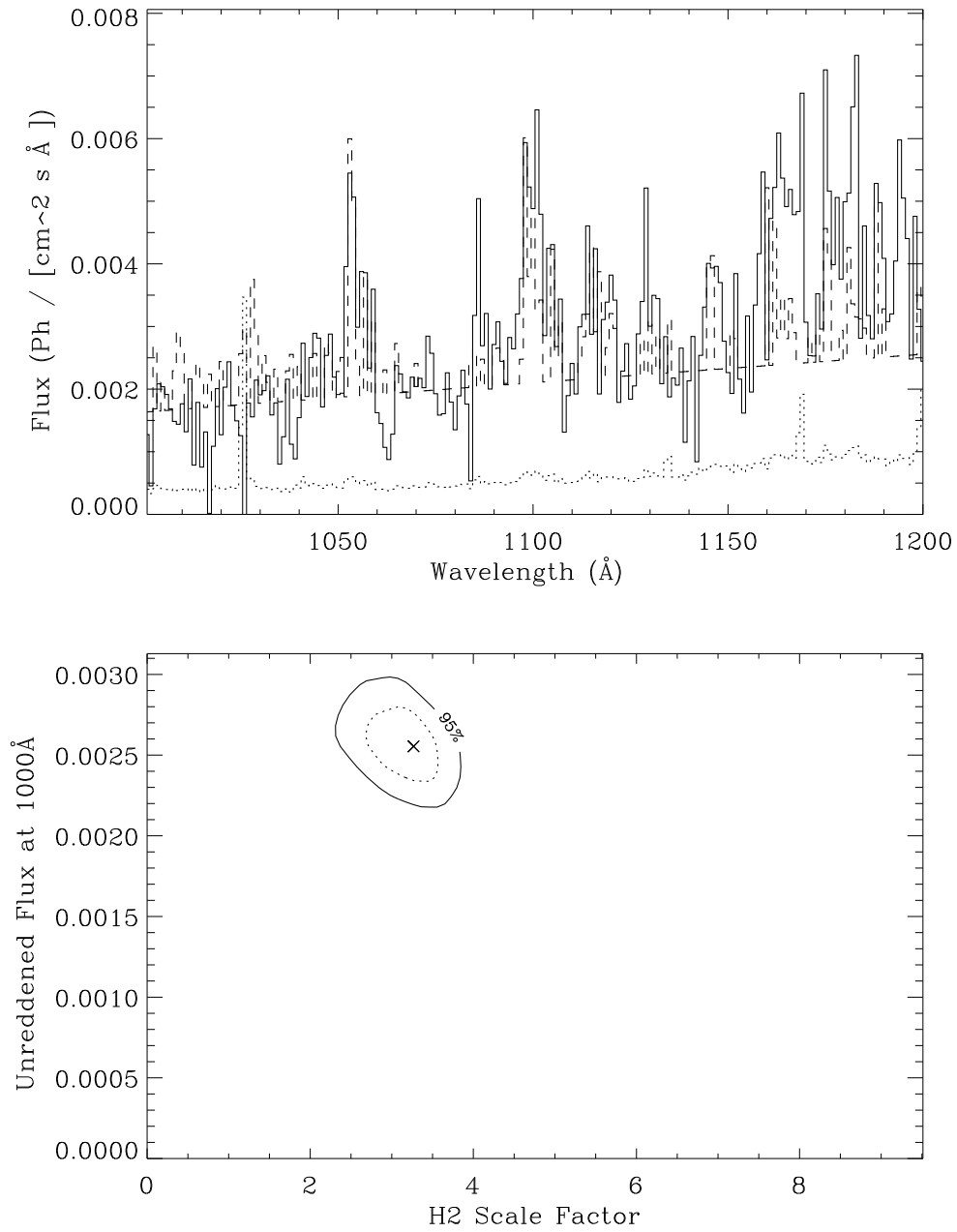


Fig. 1.— Upper panel: Observed spectrum of IC 63 (solid line), best-fit model (dashed line), and 1σ error (dotted line). Lower panel: Joint confidence interval on continuum flux at 1000 Å and H₂ scale factor. See text for definitions.